# Thin-film effects on the surface stopping power of a free electron gas

A. García-Lekue $^{(1,*)}$  and J.M. Pitarke $^{(1,2)}$ 

- (1) Materia Kondentsatuaren Fisika Saila, Zientzi Fakultatea, Euskal Herriko Unibertsitatea, 644 Posta kutxatila, 48080 Bilbo, Basque Country, Spain
  - (2) Donostia International Physics Center (DIPC) and Centro Mixto CSIC-UPV/EHU, Donostia, Basque Country, Spain

#### **Abstract**

The electronic properties of thin films present quantum-size effects, which are a consequence of the finite size of the system. Here we focus on the investigation of these effects on the electronic energy loss of charged particles moving parallel with thin metallic films. The energy loss is calculated, within linear-response theory, from the knowledge of the density-response function of the inhomogeneous electron system, which we evaluate either in the random-phase approximation or with the use of an adiabatic and local exchange-correlation kernel.

PACS: 71.45.Gm, 79.20.Rf, 34.50.Bw

Keywords: Electronic energy loss; Quantum size effects

#### 1 Introduction

The interaction of moving ions with solids has represented an active field of basic and applied physics[1, 2]. Charged particles moving near metallic surfaces loose energy as a consequence of the creation of different kind of excitations in the metal, such as electron-hole pairs and both bulk and surface plasmons[3, 4]. Also, the theoretical understanding of the electronic excitations is well known to be relevant in surface physics, as these modes are invariably involved in a variety of surface spectroscopies[5-9].

Quantum-size effects (QSE) were first investigated by Schulte[10] within a jellium model of the thin film and later by Feibelman[11], showing that the various physical properties exhibit an oscillatory behaviour as a function of the thickness of thin metallic films. These effects, which decrease as the size of the thin film increases, can be observed experimentally[12]. QSE on the surface energy and the work function have been examined recently, within a stabilized jellium model of the electron system[13].

In this paper we focus on the investigation of QSE on the energy-loss spectra of charged particles moving parallel with metallic slabs. The energy loss is calculated, within linear response theory, from the knowledge of the density-response function of the inhomogeneous electron system, which we evaluate either in the random-phase approximation or with the use of an adiabatic and local exchange-correlation kernel.

1

<sup>\*</sup> Electronic address: wmbgalea@lg.ehu.es; Fax: +34-94-464-8500

In Section 2 we present general expressions for the energy loss of charged particles moving along a definite trajectory. The results of our self-consistent calculations are presented in Section 3, and in Section 4 our main conclusions are summarized. Atomic units are used throughout, i.e.,  $e^2 = \hbar = m_e = 1$ .

## 2 Theory

We consider a recoiless particle of charge  $Z_1$  moving with constant velocity  $\mathbf{v}$  along a definite trajectory at a fixed distance z from the planar surface of a bounded three-dimensional electron gas that is translationally invariant in two directions. The energy that the moving particle looses per unit path length, i.e., the so-called stopping power of the electron system may be obtained from the gradient along the particle trajectory of the self-consistent potential set up by the particle in the electron system and evaluated at the position of the particle [14]. Within linear response theory, one finds [15]:

$$-\frac{dE}{dx} = -\frac{2}{v} Z_1^2 \int \frac{d\mathbf{q}_{\parallel}}{(2\pi)^2} \int_0^{\infty} d\omega \, \omega \, \text{Im} W(z, z; \mathbf{q}_{\parallel}, \omega) \, \delta(\omega - \mathbf{q}_{\parallel} \cdot \mathbf{v}), \tag{1}$$

where  $\mathbf{q}_{\parallel}$  is the momentum transfer in the plane of the surface,  $\omega$  represents the energy transfer, and  $W(z, z; \mathbf{q}_{\parallel}, \omega)$  is the screened interaction

$$W(z, z'; q_{\parallel}, \omega) = v(z, z'; q_{\parallel}) + \int dz_1 \int dz_2 \, v(z, z_1; q_{\parallel}) \, \chi(z_1, z_2; q_{\parallel}, \omega) \, v(z_2, z'; q_{\parallel}), \quad (2)$$

 $v(z, z'; q_{\parallel})$  and  $\chi(z, z'; q_{\parallel}, \omega)$  being two-dimensional Fourier transforms of the bare Coulomb potential and the density-response function, respectively[16].

The stopping power of the electron system can be described by means of  $P(\omega)$ , the total probability for the moving particle to exchange energy  $\omega$  with the medium:

$$-\frac{dE}{dx} = \frac{1}{v} \int_0^\infty d\omega \,\omega \,P(\omega),\tag{3}$$

where

$$P(\omega) = -\frac{Z_1^2}{\pi^2 v} \int_0^\infty dq_x \operatorname{Im} W(z, z; q_{\parallel}, \omega), \tag{4}$$

with  $q_{\parallel} = \sqrt{q_x^2 + (\omega/v)^2}$  and  $q_x$  being the momentum transfer along the particle trajectory.

The key ingredient of our energy-loss calculations is the density-response function of the electron system, which is known to satisfy the following integral equation [17]

$$\chi(z, z'; q_{\parallel}, \omega) = \chi^{0}(z, z'; q_{\parallel}, \omega) + \int dz_{1} \int dz_{2} \chi^{0}(z, z'; q_{\parallel}, \omega) 
\times \left[ v(z_{1}, z_{2}; q_{\parallel}) + f_{xc}(z_{1}, z_{2}; q_{\parallel}, \omega) \right] \chi(z_{2}, z'; q_{\parallel}, \omega),$$
(5)

where  $\chi^0(z, z_1; q_{\parallel}, \omega)$  is the density-response function of non-interacting electrons moving in the effective Kohn-Sham potential of density-functional theory (DFT)[18], and the kernel  $f_{xc}(z, z'; q_{\parallel}, \omega)$  accounts for exchange-correlation (xc) effects beyond a time-dependent Hartree approximation.

Exchange-correlation effects are usually introduced within the local-density approximation (LDA) of DFT, by replacing the xc potential at z by that of a uniform electron gas of density n(z). The xc kernel entering Eq. (5) is then set either equal to zero [this is the random-phase approximation (RPA)] or equal to the static ( $\omega = 0$ ) xc kernel

$$f_{xc}^{ALDA}(z, z'; q_{\parallel}, \omega) = \left[\frac{dv_{xc}(n)}{dn}\right]_{n=n(z)} \delta(z - z'). \tag{6}$$

This is the so-called adiabatic local-density approximation (ALDA).

We consider a jellium slab of thickness a normal to the z axis, consisting of a fixed uniform positive background of density:

$$n_{+}(z) = \begin{cases} \bar{n}, & -a \le 0\\ 0, & \text{elsewhere,} \end{cases}$$
 (7)

plus a neutralizing cloud of interacting electrons of density n(z). The positive-background charge density is  $\bar{n} = q_F^3/3\pi^2$ , where  $q_F = (9\pi/4)^{1/3}/r_s$  is the Fermi momentum and  $r_s$  is the Wigner-Seitz radius.

To compute  $\chi(z, z'; q_{\parallel}, \omega)$ , we follow the method described in Ref. [19]. We first assume that n(z) vanishes at a distance  $z_0$  from either jellium edge, and expand the one-electron wave functions in a Fourier sine series. The distance  $z_0$  and the number of sine functions kept in the expansion of the wave functions are chosen sufficiently large for our calculations to be insensitive to the precise values employed. We then introduce a double-cosine representation for the density-response function, and find explicit expressions for the screened interaction and the energy-loss probability in terms of the Fourier coefficients of the density-response function [15].

QSE are originated in the quantization of the energy levels normal to the surface. As the slab-thickness a increases new subbands for the z motion become occupied, thereby leading to oscillatory functions of a with and amplitude that decays approximately linearly with a and a period that equals  $\lambda_F/2$ ,  $\lambda_F = 2\pi/q_F$  being the Fermi wavelength. These size effects are responsible for the oscillatory behaviour of the electronic density induced in the electron system by the external probe and also for the oscillations of the energy-loss function and the stopping power with the system size. The results presented below correspond to slabs with the number n of occupied subbands in the range n = 11 - 14, for which  $a \sim 4 - 7 \lambda_F$ .

### 3 Results

We have investigated thin-film effects on the energy-loss spectra of aluminum slabs, for which  $r_s = 2.07$  and  $\lambda_F = 6.77 a_0$  ( $a_0$  is the Bohr radius,  $a_0 = 0.529 \,\text{Å}$ ). We set  $Z_1 = \pm 1$  and our results can then be used for arbitrary values of  $Z_1$ , as the energy-loss probability is, within linear-response theory, proportional to  $Z_1^2$ .

The main ingredient of our calculations is the energy-loss function  $\text{Im}W(z,z;q_{\parallel},\omega)$ . Fig. 1 shows this quantity, as obtained from Eq. (2) with use of either the RPA or the ALDA density-response function, versus the slab-thickness a and for  $z=2\,a_0$ ,  $q_{\parallel}=0.4\,q_F$ , and  $\omega=0.2\,\omega_p$  [ $\omega_p=(4\pi\bar{n})^{1/2}$  is the classical plasma frequency of a uniform electron gas of density  $\bar{n}$ ]. As a increases, new subbands for the z motion

become occupied. For  $r_s=2.07$ , the n=11,12,13,14 subbands fall below the Fermi level for  $a_n=4.95,5.46,5.96,6.46\,\lambda_F$ . When a new subband is pulled below the Fermi level, the parallel Fermi sea built upon the newly occupied subband acquires more electrons, thereby increasing the screening and decreasing the energy-loss function. However, this effect is eventually overcome by the fact that all the subbands for the z motion get deeper with increasing film thickness. When a is increased by  $\sim \lambda_F/2$ , a new subband begins to be filled and a new oscillation begins. The energy-loss function of a semi-infinite medium can then be extrapolated with the use of the following relation [20]

$$ImW = \frac{ImW[a_n] + ImW[a_n] + ImW[a_n^+]}{3},$$
 (8)

where  $a_n^- = a_n - \lambda_F/4$  and  $a_n^+ = a_n + \lambda_F/4$ .

The impact of short-range xc effects on the energy-loss function is investigated by employing the many-body kernel of Eq. (6). These effects provoke a reduction in the screening of the electron-electron interaction, thereby increasing the energy loss for all projectile trajectories. This is observed in Fig. 2, where the RPA and ALDA energy-loss function is shown as a function of the z coordinate  $[z \ge 0]$  in the vacuum, at the right-hand side of the slab] for two different values of a corresponding to a local minimum  $(a = a_{11})$  and one of the two local maxima about the minimum  $(a = a_{11})$ , and the same values of  $q_{\parallel}$  and  $\omega$  as in Fig. 1. The energy-loss function of the semi-infinite medium is also shown, by a solid line. We find that size effects become more significant as the particle moves away from the surface into the vacuum, which is due to the fact that as z increases the external field couples mainly with plasmon modes. Since these are modes characterized by their long wavelength, their behaviour depends strongly on the overall size of the system. For particles moving close to the surface the interaction has a short-range character, as the excitation of electron-hole pairs plays an increasing role.

Fig. 5 shows the RPA and ALDA probability  $P(\omega)$ , as obtained from Eq. (4) versus the slab thickness a, for an external particle with  $v = 0.5 v_0$  [ $v_0$  is the Bohr velocity,  $v_0 = 2.19 \times 10^6 \,\mathrm{ms}^{-1}$ ] and  $z = 2 \,a_0$  to exchange energy  $\omega = 0.2 \,\omega_p$  with an Al slab. This figure exhibits an oscillatory behaviour similar to that shown in Fig. 1 for the energy-loss function. In Fig. 5 we have represented the RPA and ALDA energy-loss probability  $P(\omega)$ , as a function of the energy transfer  $\omega$ , with the same values of v, z and a as in Fig. 3. As in the case of the energy-loss function, ALDA probabilities are well over those obtained in the RPA, due to the presence of short-range xc effects.

The dependence of the RPA and ALDA stopping power on the thickness a of the slab, as obtained from Eq. (1), is exhibited in Fig. 5. We have considered a charged particle moving with velocity  $v=2\,v_0$  along a definite trajectory at a fixed distance  $z=2\,a_0$  from the right edge of an Al film. For these values of z and v the ALDA stopping power is significantly larger than that obtained in the RPA. Fig. 5 shows the RPA and ALDA stopping power, as a function of the velocity, for a projectile moving at a fixed distance  $z=2\,a_0$  from the surface into the vacuum. As the velocity increases the energy-loss spectrum of charged particles moving outside the solid is dominated by long-wavelength excitations and short-range xc effects, not included in the RPA, tend to become less important.

.

#### 4 Conclusions

We have investigated quantum-size effects on the energy-loss spectra of charged particles moving parallel with metallic slabs, in the framework of linear-response theory.

We have found that the quantization of the energy levels normal to the surface yields a neat oscillatory behaviour of the screened interaction, the energy-loss probability and the stopping power, as a function of the thickness of the slab. The amplitude of these oscillations is found to decay approximately linearly with the slab thickness and their period is found to equal  $\sim \lambda_F/2$ . We have also presented self-consistent calculations for a semi-infinite medium, which have been obtained from finte-slab calculations with the use of the extrapolation formula given in Ref. 20.

Our results indicate that size effects become more significant as the particle moves away from the surface into the vacuum, where long-wavelength excitations play an important role. As for the impact of short-range xc effects on the various magnitudes that characterize the interaction of charged particles with metallic films, we have found that they increase the energy-loss probability, due to the reduction that these effects provoke in the screening of electron-electron interactions.

A more detailed presentation of our self-consistent calculations of the energy-loss spectra of charged particles moving near a semi-infinite electron system will be published elsewhere [15].

# 5 Acknowledgments

We acknowledge partial support by the University of the Basque Country, the Basque Unibertsitate eta Ikerketa Saila, and the Spanish Ministerio de Educación y Cultura.

### References

- [1] D. H. Schneider and M. A. Briere, Phys. Scr. **53**, 228 (1996).
- [2] A. Arnau et al, Surf. Sci. Rep. bf 27, 113 (1997).
- [3] D. Pines, Solid State Phys. 1, 367 (1955).
- [4] R. H. Ritchie, Phys. Rev. **106**, 874 (1957).
- [5] H. Raether, in Excitations of Plasmons and Interband Transitions by Electrons, edited by G. Höhler, Springer Tracks in Modern Physics, Vol. 88 (Springer, Berlin, 1980).
- [6] P. E. Batson, Phys. Rev. Lett. 49, 936 (1982).
- [7] H. Kohl, Ultramicroscopy **11**, 53 (1983).
- [8] R. H. Ritchie and A. Howie, Philos. Mag. A 58, 753 (1988).
- [9] D. W. McComb and A. Howie, Nucl. Instrum. Methods B **96**, 569 (1995).
- [10] F. K. Schulte, Surf. Sci. **55**, 427 (1976).

- [11] P. J. Feibelman, Phys. Rev. B 27, 1991 (1983).
- [12] R. C. Jaklevic and J. Lambe, Phys. Rev. B 12, 4146 (1975).
- [13] I. Sarria, C. Henriques, C. Fiolhais, and J. M. Pitarke, Phys. Rev. B **62**, 1699 (2000).
- [14] P. M. Echenique, F. Flores, and R. H. Ritchie, Solid State Phys. 43, 230 (1990).
- [15] A. García-Lekue and J. M. Pitarke, to be published.
- [16] P. Nozieres and D. Pines, *The theory of quantum liquids* (Benjamin, New York, 1966).
- [17] E. K. U. Gross, J. F. Dobson, and M. Petersilka, in *DensityFunctional Theory II*, Vol. 181 of *Topics in Current Chemistry*, edited by R. F. Nalewajski (Springer, Berlin, 1996).
- [18] W. Kohn and L. J. Sham, ibid. 140, A11333 (1965); P. Hohenberg and W. Kohn, Phys. Rev. 136 B864 (1964).
- [19] A. G. Eguiluz, Phys. Rev. Lett. **51**, 1907 (1983); Phys. Rev. B **31**, 3303 (1985).
- [20] J. M. Pitarke and A. G. Eguiluz, Phys. Rev. B 57, 6329 (1998); J. M. Pitarke and A. G. Eguiluz, Phys. Rev. B (in press).
- Figure 1: The RPA and ALDA energy-loss function  $\text{Im}W(z,z;q_{\parallel},\omega)$ , as a function of the slab thickness a, for  $q_{\parallel}=0.4\,q_F$ ,  $\omega=0.2\,\omega_p$ , and  $z=2\,a_0$ . Dashed lines represent the infinite-width limit, as obtained from Eq. (8). The damping parameter in the evaluation of the density-response function of non-interacting Kohn-Sham electrons has been taken to be  $\eta=\omega_p/10$ .
- Figure 2: The RPA and ALDA energy-loss function  $\text{Im}W(z, z; q_{\parallel}, \omega)$ , as a function of the z coordinate, for two different values of the slab width and the same values of  $q_{\parallel}$ ,  $\omega$  and  $\eta$  as in Figure 1. Thick solid lines represent the infinite-width limit of Eq. (8). Dashed and thin-solid lines represent the energy-loss function for  $a = a_{11}$  and  $a = a_{11}^-$ , respectively.
- Figure 3: The RPA and ALDA energy-loss probability  $P(\omega)$ , as a function of the slab thickness a, for  $\omega = 0.2 \omega_p$ ,  $z = 2 a_0$ ,  $v = 0.5 v_0$ , and  $\eta = \omega_p/10$ . Dashed lines represent the infinite-width limit, which is obtained as in Eq. (8) with P instead of ImW.

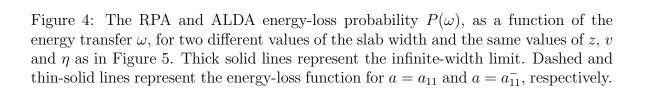


Figure 5: The RPA and ALDA stopping power, -(dE/dx), as a function of the slab thickness a, for  $z=2\,a_0$ ,  $v=0.5\,v_0$ , and  $\eta=\omega_p/10$ . Dashed lines represent the infinite-width limit, which is obtained as in Eq. (8) with -(dE/dx) instead of ImW.

Figure 6: The RPA and ALDA stopping power, -(dE/dx), as a function of the velocity v, for two different values of the slab width and the same values of z and  $\eta$  as in Figure 5. Thick solid lines represent the infinite-width limit. Dashed and thin-solid lines represent the energy-loss function for  $a=a_{11}$  and  $a=a_{11}^-$ , respectively.

